Spatial distribution of the microzooplankton communities in the northern South China Sea: Insights into their function in microbial food webs

Jinpeng Yang [a,b,*], Zijian Chen [c], Dongxing Chen [a], Dapeng Xu [d,e]

[a] School of Marine Sciences, Sun Yat-Sen University, Guangzhou 510006, China
[b] Guangdong Provincial Key Laboratory of Marine Resources and Coastal Engineering, Guangzhou 510006, China
[c] South China Sea Marine Survey and Technology Center, SOA, Guangzhou 510006, China
[d] State Key Laboratory of Marine Environmental Science, College of Ocean and Earth Sciences, Xiamen University, Xiamen 361102, China
[e] Fujian Key Laboratory of Marine Carbon Sequestration, Xiamen University, Xiamen 361102, China

ARTICLE INFO

ABSTRACT

The spatial distribution of microzooplankton in the northern South China Sea was investigated in March 2016. Microzooplankton communities were dominated by cyclotrichids, aloricate oligotrichs, and choreotrichs within ciliates and the order Gymnodiniales within dinoflagellates. Microzooplankton abundance varied between 60 and 166,520 cells L^{-1}, with higher values in the coastal diluted water, and microzooplankton biomass exhibiting a similar pattern. High densities of *Akashiwo* cf. *sanguinea* were found in the upper waters along the coast, and mixotrophs dominated the communities in all the water masses. A canonical analysis of principal coordinates showed that the spatial patterns of microzooplankton communities could be clearly discriminated in the different water masses. Our findings provide insights into the functioning of microzooplankton and the potential risk of harmful *Akashiwo* cf. *sanguinea* algal blooms in coastal waters. In addition, our study provides evidence for using microzooplankton communities as potential indicators of water masses in complex marine systems.

1. Introduction

Microzooplankton, referring to the size fraction of heterotrophic planktonic organisms between 20 and 200 μm, are taxonomically diverse and form a substantial proportion of microbial food webs as an important structural and functional group in pelagic ecosystems (Burkill et al., 1993; Garrison et al., 2005; Löder et al., 2011). They have been recognised as major consumers of primary producers, accounting for 60–75% of the mortality of phytoplankton producers across a spectrum of open ocean and coastal systems (Landry and Calbet, 2004). Within microzooplankton, ciliates and dinoflagellates are the most important components (Capriulo et al., 1991) and have received increasing attention since the 'microbial loop' was introduced (Azam et al., 1983). Ciliates are commonly referred to as primary grazers of pico- and nanoplankton (Sherr and Sherr, 1987; Burkill et al., 1993), which are the dominant size fractions in terms of biomass and primary productivity in pelagic ecosystems (Wickham et al., 2011; Sherr et al., 2013). Compared to ciliates, dinoflagellates have a wider food spectrum, including phototrophic and heterotrophic bacteria (Jeong et al., 2005; Jeong et al., 2008), microalgae (Nakamura et al., 1995; Li et al., 2000; Berge et al.,

2008; Yoo et al., 2009), heterotrophic nanoflagellates (Jeong et al., 2007), other dinoflagellates (Tillmann, 2004), ciliates (Hansen, 1991), early naupliar stages, and even adult forms of metazoans (Jeong, 1999). Both ciliates and dinoflagellates serve as important food sources for metazoans, such as copepods (Gifford, 1991; Löder et al., 2011). Furthermore, a substantial proportion of microzooplankton are mixotrophic and may function as primary producers via inherited plastids, algal ecto- or endosymbionts, or plastids from ingested algal prey (Johnson, 2011; Stoecker et al., 2017). Thus, microzooplankton play a crucial role in the functioning of marine ecosystems (Sherr and Sherr, 1987; Gifford, 1991), and variations in the taxonomic composition of microzooplankton communities can have a significant effect on key ecosystem functions, such as primary and secondary production, and nutrient cycling (Levinsen and Nielsen, 2002). Compared to larger and more motile zooplankton, microzooplankton are more susceptible to physical factors (e.g. freshwater intrusion and water currents) in spatial distribution because of their limited motility (Reid and Stewart, 1989). Thus, it is essential to examine the spatial distribution patterns of microzooplankton communities in different water bodies of various marine regions, especially those with complex dynamic interactions.

---

* Corresponding author at: School of Marine Sciences, Sun Yat-Sen University, Guangzhou 510006, China.
  E-mail address: yangjp8@mail.sysu.edu.cn (J. Yang).

The South China Sea (SCS), covering an area of approximately 3.3 million km^2, is one of the largest marginal seas in the western Pacific Ocean (Liang et al., 2008). It is characterised by a tropical maritime climate and has characteristics typical of a monsoon climate, with the southwest monsoon prevailing in summer and the northeast monsoon prevailing in winter (Liu et al., 2010; Zheng et al., 2012). The northern SCS (nSCS) has diverse ecological environments, including coastal zones that are rich in nutrients and low in salinity due to the effect of freshwater intrusion, continental shelves with moderate nutrients and salinity, continental slopes, and open seas with oligotrophic conditions and high salinity (Liu et al., 2010). The hydrological conditions of the nSCS are extremely complex and dynamic, especially in coastal and continental shelf areas, which are strongly influenced by runoff from the Pearl River, water stratification, thermocline, seasonal upwelling, and coastal currents formed by monsoons and topographies (Gan et al., 2010; Zheng et al., 2012). Over the past 30 years, intensive marine aquaculture development and rapid industrialisation along the coast of the nSCS have placed heavy stress on the marine environment, and frequent occurrences of harmful algal blooms (HABs) have caused enormous economic losses and adverse effects on human health and marine ecosystems in this region (Tang et al., 2003; Qi et al., 2004; Wang et al., 2008).

Although the importance of microzooplankton in microbial food webs is being increasingly recognised, studies based on quantitative abundance and biomass data with high taxonomic resolution, particularly in the nSCS, are still limited. Some investigations have been conducted on planktonic ciliates in this region, yet most studies have focused on ciliate abundance and species diversity in tintinnids (Yu et al., 2014; Wang et al., 2019). For aloricate oligotrich ciliates, which usually dominate planktonic ciliate communities in coastal waters and open oceans (Yang et al., 2015, 2020a; Sun et al., 2017; Huang et al., 2020), less information is available on their distribution and diversity in the nSCS (Liu et al., 2010; Sun et al., 2019), as they are typically small, fragile, and difficult to identify without taxonomic expertise (Song et al., 2009). Moreover, investigations on dinoflagellates in the nSCS have mainly treated them as phytoplankton rather than microzooplankton (Ke et al., 2011; Wei et al., 2018; Dai et al., 2020), even though many heterotrophic dinoflagellates (HTDs) have been reported and many phototrophic dinoflagellates which had previously been thought to be exclusively autotrophic have been revealed to be capable of ingesting prey, i.e. mixotrophic dinoflagellates (MTDs) (Stoecker, 1999; Jeong et al., 2010). As a result, little is known about the spatial distribution patterns and community structure of the whole microzooplankton community in the nSCS, which impedes our understanding of their ecological functions in this ecosystem. In addition, toxic or harmful algae have occupied an increasing proportion of bloom-forming species in the coastal waters of China (Glibert et al., 2018). It is known that most toxic or harmful bloom-forming algae are MTDs (Jeong et al., 2010), and the predator–prey relationships within microzooplankton communities could provide insights into the dynamics of red tides dominated by MTDs (Yang et al., 2019).

To improve our knowledge in this context, microzooplankton samples and other abiotic parameters were collected on a multidisciplinary expedition during the early spring in 2016 in the western nSCS, where the physico-chemical processes are sophisticated owing to the influence of runoff from the Pearl River Estuary and the complex coastlines of the Leizhou Peninsula and Hainan Island (Wu and Li, 2003), providing an ideal environment for examining microzooplankton assemblages in marine systems with dynamic environmental variations. The main aim of the present study was to characterise the spatial distribution patterns of microzooplankton communities in the coastal and continental shelf areas of the nSCS. The objectives were to 1) reveal the species composition and spatial distribution patterns of microzooplankton communities in the nSCS; 2) compare the differences in the abundance and biomass of the communities between different water bodies; and 3) provide insights into their function in microbial food webs.

2. Materials and methods

2.1. Study area and sample collection

A multidisciplinary survey was conducted onboard R/V Haidiao VI at 47 stations in the coastal and continental shelf areas of the western nSCS from 28 February to 5 March 2016 (Fig. 1). The water depths at all the stations ranged from 8 m to nearly 400 m. At each station, the vertical profiles of water temperature and salinity (from the surface down to the bottom) were measured with probes equipped on a Seabird (SBE 911plus) CTD profiler. In addition, 90 samples were collected to determine the microzooplankton communities using 10 L Niskin rosette samplers from 2 to 6 depths at alternate stations (21 biological stations), with water depths ranging from 8 m (St. 1) to 210 m (St. 9) (Table S1). The water samples (500 mL) from each depth were immediately fixed with acid Lugol's iodine solution (2% final concentration) and stored in cold and dark conditions until analysis (Yang et al., 2020b).

2.2. Identification and enumeration of microzooplankton

Microzooplankton abundance and taxonomic composition were evaluated by settling subsamples (25, 50, or 100 mL, depending on the cell density) in Utermöhl sedimentation chambers for at least 24 h and examining the whole chamber at a 200-fold magnification under an inverted microscope (Mingmei MI12). Following this procedure, at least 10 individuals of the dominant taxa and fewer of rare taxa were enumerated in each subsample. The biovolume of each taxon was determined following the geometric models described by Hillebrand et al. (1999) based on the measurement of cell dimensions with an ocular micrometre. The average biovolume of each taxon was estimated from at least 20 cells for dominant taxa and all cells for rare taxa and then converted into carbon biomass using a conversion factor of 0.19 pg C μm^{-3} for ciliates (Putt and Stoecker, 1989). The carbon content of each dinoflagellate taxon was obtained using the equation (pg C cell^{-1} = $0.760 \times V^{0.819}$) given by Menden-Deuer and Lessard (2000).

The identification of tintinnids was based on lorica features and species descriptions from Kofoid and Campbell (1929). Other ciliate taxa were identified mainly according to Montagnes and Lynn (1991) and Song et al. (2009). Dinoflagellate identification was mainly based on Kraberg et al. (2010). Some ciliates and dinoflagellates were only identified to the genus level or were placed into different size groups because of difficulties that can occur with the identification of microzooplankton after fixation with acid Lugol's solution. The taxonomic systematics applied in this study followed Löder et al. (2012). Based on trophic status, microzooplankton were categorised into three groups: red *Mesodinium* spp. (*Mesodinium rubrum* and *M. major*), which are strongly autotrophic mixotrophs, other mixotrophs, and heterotrophs (Löder et al., 2012; Yang et al., 2020b). The equivalent spherical diameter (ESD) of each ciliate taxon was calculated based on the biovolume to evaluate the size-fractionated composition of ciliate communities, in which red *Mesodinium* spp. were excluded as they tend to rely more on phototrophy than phagotrophy owing to their relatively low ingestion rates and long survival time without prey (Stoecker et al., 2017).

2.3. Data processing

The temperature–salinity (T–S) diagram (Sun et al., 2020) was applied to delineate water masses, and the classification of water masses was based on Li et al. (2002). A one-way analysis of variance (ANOVA) was used to assess the differences in microzooplankton abundance, carbon biomass, and trophic composition among different water bodies, and the least significant difference (LSD) test of mean comparisons between groups was performed using SPSS (Version 19, SPSS Inc.). The spatial differences in microzooplankton communities were demonstrated using the PERMANOVA+ submodule CAP (canonical analysis of
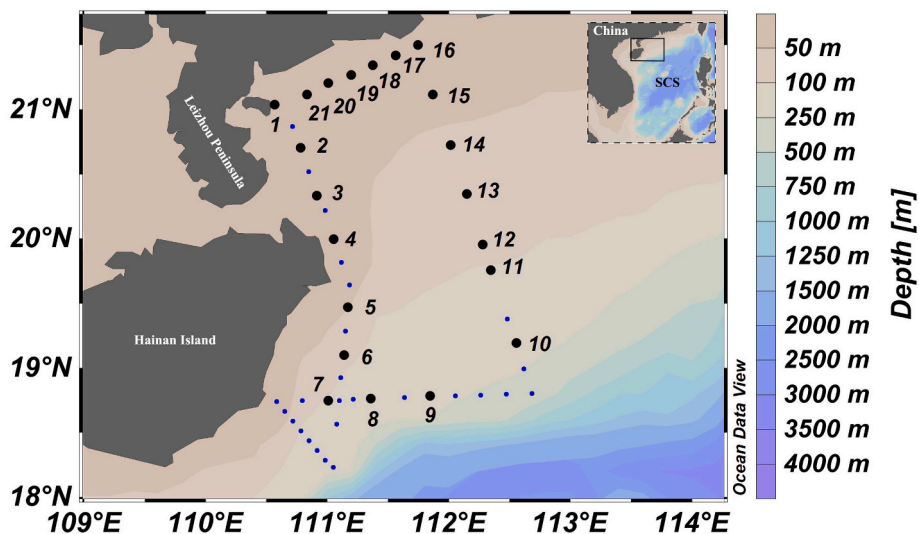
Fig. 1. Sampling stations in the western northern South China Sea (nSCS) in March 2016 (blue circles: physical stations; black circles: physical and biological stations). (For interpretation of the references to colour in this figure legend, the reader is referred to the web version of this article.)
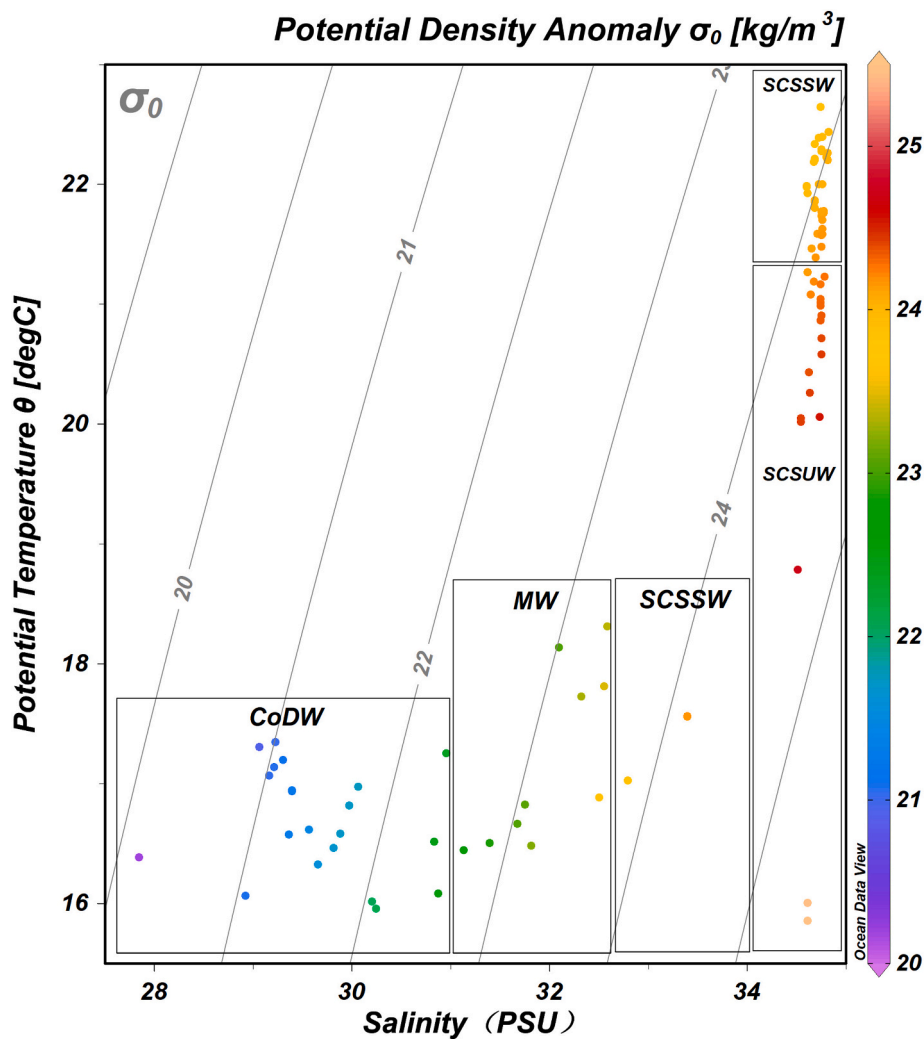

Fig. 2. Four water masses identified based on properties of temperature and salinity. The lines across the panel represent isodensity. CoDW: coastal diluted water; MW: mixing water; SCSSW: the South China Sea (SCS) surface water; SCSUW: the SCS subsurface water.

principal coordinates) with Bray–Curtis similarities based on the square-root transformed data of microzooplankton abundance (Clarke and Gorley, 2006; Anderson et al., 2008). A permutational multivariate ANOVA (PERMANOVA) was conducted to test the differences among groups (Anderson et al., 2008). Community diversity parameters (the Shannon–Weiner index (H'), Pielou's evenness (J'), and Margalef's richness (d)) were computed using the PRIMER v 6.1 package (Clarke and Gorley, 2006). The contribution of each species to the dissimilarity between different groups was examined using the similarity percentage analysis (SIMPER) programme (Clarke and Gorley, 2006). Geographical maps were created using the ODV software (Schlitzer, Ocean Data View) and other figures were produced in SigmaPlot 12.5 (Systat Software Inc., San Jose, CA, USA). A significance level of 0.05 was chosen for the statistical analyses.

3. Results

3.1. Hydrologic structure of water masses

According to the *T–S* plot, four water masses were identified: the coastal diluted water (CoDW) with a salinity lower than 31.00 and temperature range from 15.96 to 17.35 °C, the nearshore mixing water (MW) with a salinity between 31.00 and 32.59 and temperature range from 16.45 to 18.32 °C, the SCS surface water (SCSSW) with a salinity higher than 32.59 and temperature range from 17.03 to 22.65 °C, and the SCS subsurface water (SCSUW) with a salinity higher than 34.50 and temperature range from 15.89 to 21.79 °C (Fig. 2; Table S1). The surface temperature exhibited an increasing trend from the coastal areas to the continental shelf areas (Fig. 3A), while the bottom temperature showed a different pattern, with temperatures in the southeast of the Hainan

Island and the inner shelf higher than those in the northern coast and outer shelf areas (Fig. 4A). The surface salinity exhibited a similar pattern to that of the bottom layer, both of which increased from the coastal areas in the north southward to the continental shelf areas (Figs. 3B, 4B). Vertically, the temperature generally decreased with increasing water depth (Figs. S1A, S2A), while salinity in the water column was quite consistent, except in the coastal areas (Figs. S1B, S2B).

3.2. Spatial variations in species number, abundance, and carbon biomass

The taxonomic composition of the microzooplankton communities is summarised in Table S2. A total of 81 different taxa of ciliates and dinoflagellates representing 46 genera and 13 orders were recorded during the survey. Of these, 57 ciliate species were identified, including 24 species of tintinnids, 18 species of aloricate oligotrichs and choreotrichs, and 15 species of other ciliates. Twenty-four species of dinoflagellates were recorded, with 8 species in the order Gymnodiniales, 6 species in the order Gonyaulacales, 5 species in the order Peridiniales, and 5 species in other orders. The number of microzooplankton species in the samples ranged from 3 to 30, with the highest richness observed at the 30 m layer of St. 8, and the minimum at the bottom layer of St. 10 (Table S1). Among the water masses, the average species numbers ($\pm$ SD) in the CoDW, MW, SCSSW, and SCSUW were ca. 20 $\pm$ 5, 19 $\pm$ 4, 20 $\pm$ 4, and 14 $\pm$ 6, respectively (Fig. 5A). There were significant differences among the different water masses in terms of species number (one-way ANOVA, $F = 7.753$, $P < 0.001$). Based on the LSD test, the species numbers in the CoDW, MW, and SCSSW were significantly higher than those in the SCSUW, while there was no significant difference between each pair of the CoDW, MW, and SCSSW (Fig. 5A).

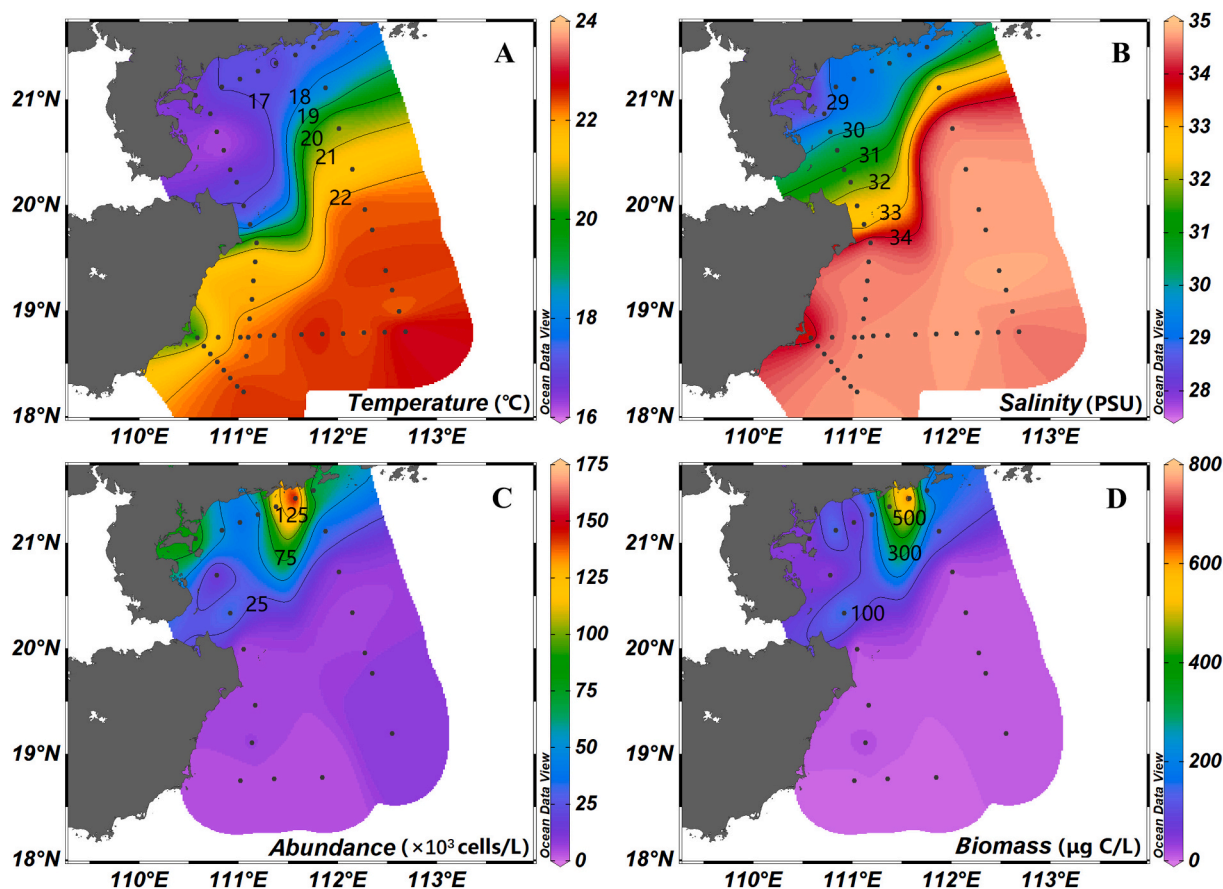The horizontal distribution of microzooplankton abundance

Fig. 3. Horizontal distribution of surface temperature (A), salinity (B), microzooplankton abundance (C) and carbon biomass (D) in March 2016 in the coastal and continental shelf areas of the western northern South China Sea (nSCS).

Fig. 4. Horizontal distribution of bottom temperature (A), salinity (B), microzooplankton abundance (C) and carbon biomass (D) in March 2016 in the coastal and continental shelf areas of the western northern South China Sea (nSCS).
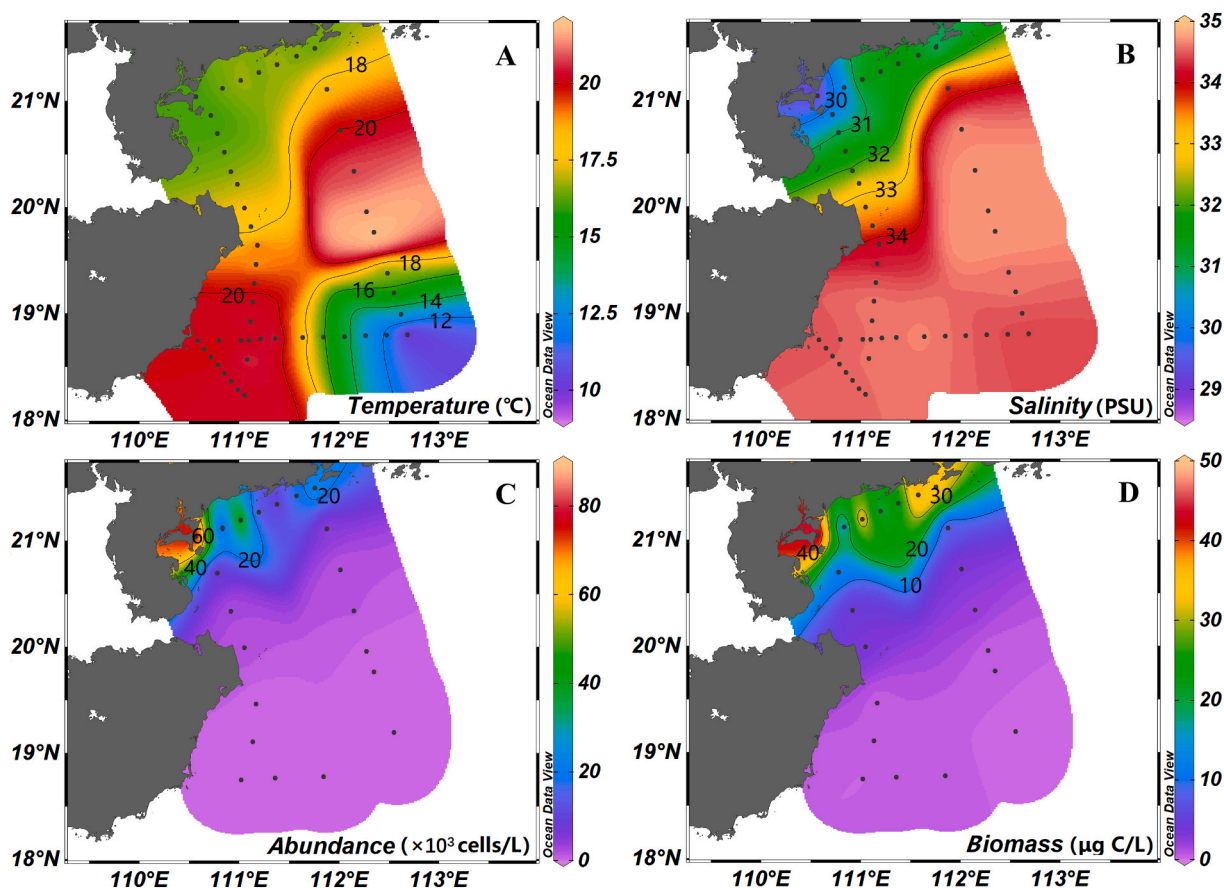
exhibited an obvious decreasing trend from coastal to continental shelf areas (Figs. 3C, 4C). The average surface microzooplankton abundance (± SD) was approximately $33.25 \pm 44.64 \times 10^3$ cells L^{-1}, and a conspicuous patch (166.52×10^3 cells L^{-1}) was found in the middle of the coastal region (Fig. 3C). The average microzooplankton abundance at the bottom layer was approximately $10.66 \pm 20.05 \times 10^3$ cells L^{-1}, and an obvious patch (82.32×10^3 cells L^{-1}) was found in the western side of the coastal area because of the high abundance of the strongly autotrophic mixotroph *M. rubrum* (81.44×10^3 cells L^{-1}) (Fig. 4C). Microzooplankton carbon biomass ranged from 4.22 to 725.34 µg C L^{-1} at the surface and 0.12 to 47.32 µg C L^{-1} at the bottom, and both exhibited similar patterns as those of microzooplankton abundance (Figs. 3D, 4D). Vertically, there was a generally decreasing trend with water depth in terms of both microzooplankton abundance and carbon biomass (Figs. S1C, D, S2C, D). Most notably, a high abundance of the MTD *Akashiwo* cf. *sanguinea* was found in the upper waters along the coast, and the maximum abundance and carbon biomass reached 126.16×10^3 cells L^{-1} and 682.40 µg C L^{-1} in the surface water of St. 17, respectively (Fig. S3A, B).

Among the water masses, the average abundance and carbon biomass in the CoDW ($45.39 \pm 42.00 \times 10^3$ cells L^{-1}, 112.72 ± 178.53 µg C L^{-1}, respectively) were much higher than those in the MW ($8.92 \pm 9.12 \times 10^3$ cells L^{-1}, 27.25 ± 36.81 µg C L^{-1}, respectively), SCSSW ($3.94 \pm 2.30 \times 10^3$ cells L^{-1}, 6.27 ± 3.98 µg C L^{-1}, respectively), and SCSUW ($1.40 \pm 1.57 \times 10^3$ cells L^{-1}, 1.92 ± 2.13 µg C L^{-1}, respectively) (Fig. 5B, C). There were significant differences among the water masses in terms of both abundance (one-way ANOVA, $F = 64.406$, $P < 0.001$) and carbon biomass (one-way ANOVA, $F = 23.899$, $P < 0.001$). According to the LSD test, there were significant differences between each pair of water masses, except between the MW and SCSSW in terms of

both abundance and carbon biomass (Fig. 5B, C), and between the SCSSW and SCSUW in terms of carbon biomass (Fig. 5C).

3.3. Spatial patterns in microzooplankton community structures

Ninety samples from the four water masses were discriminated and plotted using a canonical analysis of principal coordinates (CAP). The results demonstrated that the spatial distribution patterns of microzooplankton communities in different water masses could be well discriminated (Fig. 6). A PERMANOVA test showed a significant effect of the water mass (*pseudo-F* = 13.074, $P = 0.001$), and pair-wise comparisons in the PERMANOVA test showed strong evidence against the null hypothesis, suggesting that the microzooplankton communities in the four water masses differed from one another ($P < 0.05$) (Table 1). The spatial distributions of species number, abundance, and three diversity indices of microzooplankton communities in the samples from different water masses are shown in Fig. 6A. The vectors of species number and abundance were closely related to the sample clouds from the MW, SCSSW, and CoDW. The vectors of the Shannon–Weiner diversity index (*H'*), Margalef's richness (*d*), and Pielou's evenness (*J'*) point to sample clouds from the SCSSW (Fig. 6A).

The SIMPER analysis revealed that the microzooplankton community structures differed between the samples from different water masses at high dissimilarity levels (Table S3). The dominant species revealed by the SIMPER analysis were the main contributors to the dissimilarity between each pair of water masses because of the variations in their abundance and/or occurrence. Vector overlays of these species showed that most of the vectors pointed to the sample clouds of CoDW and SCSSW (Fig. 6B). Among these species, some commonly occurred in nearly all the samples from the four water masses, such as *Strobilidium*
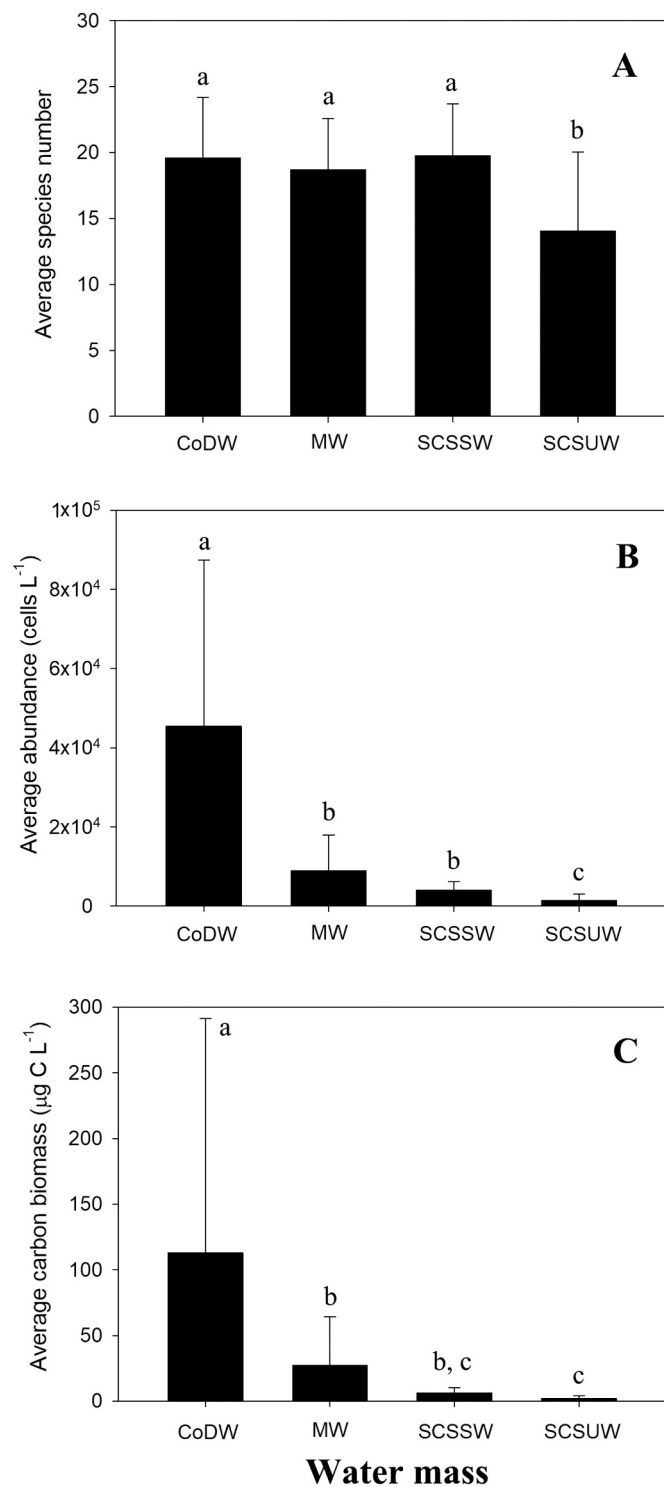
Fig. 5. Average species number (A), abundance (B) and carbon biomass (C) of microzooplankton in different water masses of the western northern South China Sea (nSCS). Error bars represent standard deviations (SD) and different lowercase letters indicate significant differences ($P < 0.05$) between the water masses.
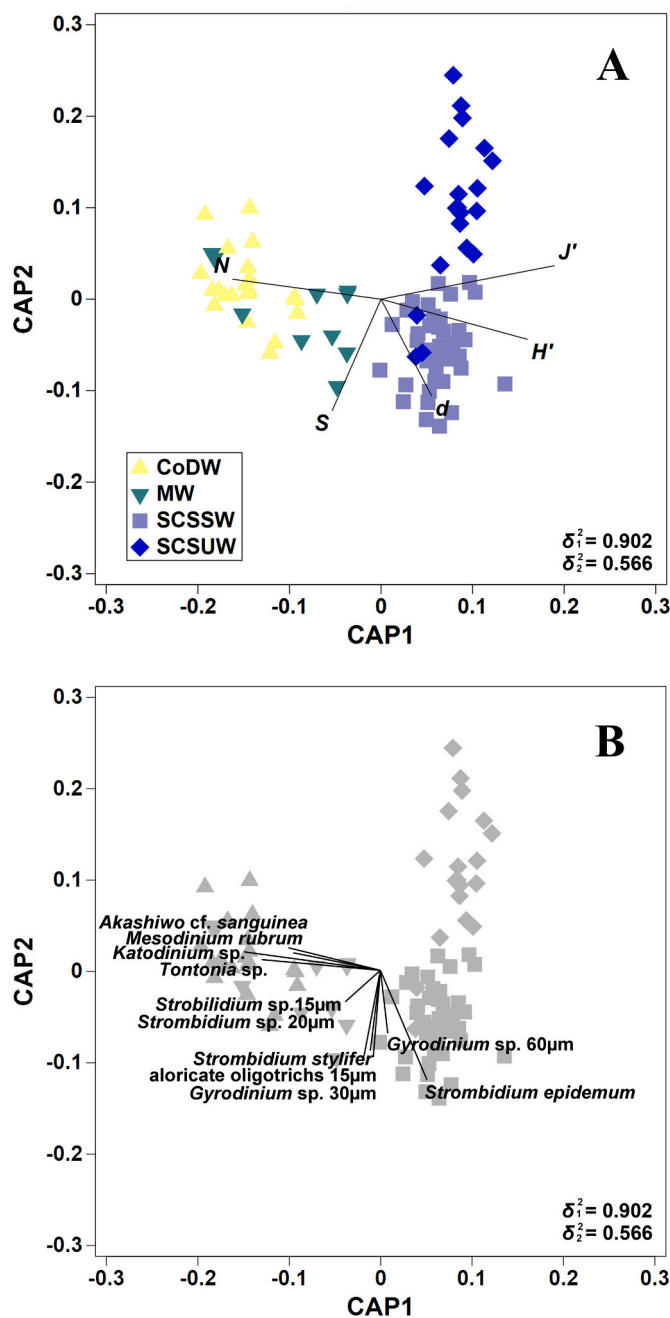

Fig. 6. Canonical analysis of principal coordinates (CAP) on Bray–Curtis similarities of 90 samples from different water masses, with community indices (A), and dominant species contributing to the dissimilarities between the water masses (B). *S*: species number; *N*: total individuals; *d*: Margalef richness; *H'*: Shannon–Weiner species diversity; *J'*: Pielou's evenness.

sp. 15 μm, aloricate oligotrichs 15 μm, and *Tontonia* sp. (Table S2). *Strombidium epidemum*, *S. stylifer*, and *Gyrodinium* spp. (30 and 60 μm) mainly occurred in the samples from the SCSSW, with higher abundance than that in the other water masses (Fig. 6B). *Mesodinium rubrum* and *Katodinium* sp. frequently occurred in the CoDW, MW, and SCSSW and were more abundant in the CoDW, while *Akashiwo* cf. *sanguinea* only

occurred in the CoDW and MW, with a higher abundance in the CoDW (Fig. 6B). In addition, some rare species only occurred in the SCSSW and SCSUW, such as *Amphorides* sp. and *Salpingella* sp., and *Dadayiella cuspis*, *D. ganymedes*, *Dictyocysta duplex*, *Eutintinnus tenue*, *Parundella* spp., and *Salpingacantha unguiculata* only occurred in the SCSSW.

The abundance compositions of ciliates, dinoflagellates, different functional groups in the microzooplankton communities, and different size groups in the ciliate communities (excluding red *Mesodinium* spp.) in the water masses are shown in Fig. 7. In the CoDW and MW, the average abundance of ciliates were lower than that of dinoflagellates, yet it was higher in the SCSSW and SCSUW (Fig. 7A, C). Cyclotrichids contributed to approximately 65% of the total ciliate abundance in the

Table 1

Results of PERMANOVA based on Bray-Curtis similarities derived from square-root transformed microzooplankton abundances among (F) and between (pair-wise tests) different water masses in the western nSCS. (CoDW: coastal diluted water; MW: mixing water; SCSSW: the SCS surface water; SCSUW: the SCS subsurface water).

	df	MS	F	P
PERMANOVA among water masses				
Water mass	3	16,978	13.074	0.001
Residual	86	1298.6		
Total	89			

	df	t	P
Pair-wise tests			
CoDW & MW	29	1.871	0.001
CoDW & SCSSW	56	4.994	0.001
CoDW & SCSUW	41	4.378	0.001
MW & SCSSW	45	2.811	0.001
MW & SCSUW	30	2.760	0.001
SCSSW & SCSUW	57	3.051	0.001

CoDW (Fig. 7A, B) owing to the high abundance of *M. rubrum* in the waters. Aloricate oligotrichs and choreotrichs contributed to approximately 84% and 77% of the total ciliate abundance in the SCSSW and SCSUW, respectively, and also dominated the ciliate communities together with cyclotrichids in the MW (58% and 34%, respectively). The species of dinoflagellates in the order Gymnodiniales had absolute predominance in the communities, contributing to 82–99% of the total dinoflagellate abundance (Fig. 7C, D). For trophic composition, the mixotrophs dominated the communities in all the water masses, contributing to 43–60% of the total microzooplankton abundance (Fig. 7E, F). There were significant differences among the water masses in terms of their trophic compositions (one-way ANOVA, $P < 0.05$). According to the LSD test, the percentage of red *Mesodinium* spp. in the CoDW (27%) was significantly higher than that in the SCSSW and SCSUW, while no significant difference was detected between the CoDW and MW (Fig. 7F). The percentage of mixotrophs in the SCSSW (60%) was significantly higher than that in the CoDW and MW, while no significant difference was detected between the SCSSW and SCSUW (Fig. 7F). There was only a significant difference between the CoDW (30%) and SCSUW (40%) in terms of the proportion of heterotrophs (Fig. 7F). Concerning size-fractionated compositions, small-sized ciliates (10–20 μm) dominated the ciliate communities in all the water masses, especially in the CoDW (83%), while large-sized ciliates (>40 μm) made up a higher proportion in the MW (16%) than in the other water masses (Fig. 7G, H).

4. Discussion

4.1. Spatial distribution of microzooplankton in the nSCS

The ciliate abundance and biomass recorded in this study showed a wide range (20–88,620 cells L^{-1}, 0.004–43.476 μg C L^{-1}), with the maxima being much higher than that commonly reported in the nSCS. The high number of ciliates in our study was mainly due to highly abundant nano-sized ciliate *Strobilidium* sp. 15 μm (max. 3.65×10^4 cells L^{-1}) and the strongly autotrophic mixotroph *M. rubrum* (max. 8.79×10^4 cells L^{-1}), which are mainly distributed in the upper waters of coastal regions. *Mesodinium rubrum* has a worldwide distribution and is well known as a red-tide former in coastal temperate waters (Stoecker et al., 2017). It often forms red tides in the German Bight during late spring and summer, with the highest density being up to 3.18×10^4 cells L^{-1} (Yang et al., 2015). In the nSCS, red tides resulting from *M. rubrum* were not observed until 1990, and since then, they have been recorded infrequently in this region (Wang et al., 2008). This species fulfils its

cellular carbon requirements mainly via phototrophic nutrition by using plastids sequestered from cryptophyte prey. In addition, this species tends to rely more on phototrophy than heterotrophy, based on their low ingestion rates and long survival time without prey (Johnson, 2011; Stoecker et al., 2017). Therefore, the high numbers of *M. rubrum* in the nSCS may be attributed to sufficient inorganic nutrients in coastal waters and suitable temperatures and light conditions during early spring (Johnson, 2011). Moreover, the species richness of tintinnids and their proportion in the ciliate communities in our study were higher than those reported by Yu et al. (2014), in which tintinnids were rarely detected and only made up approximately 1.7% of the total ciliate abundance in winter in the nSCS. These findings suggest that there may be significant annual variations in the ciliate communities in the nSCS, as revealed in the southern North Sea (Yang et al., 2015), and the effect of such variations on the functioning of the microbial food web in the nSCS ecosystem deserves further attention.

Dinoflagellates exhibited much wider ranges than ciliates in terms of both abundance and biomass (20–150,000 cells L^{-1}, 0.07–698.16 μg C L^{-1}), with an average abundance (6993 cells L^{-1}) being higher than that reported by Ke et al. (2011) and Wei et al. (2018) in the nSCS in summer (1190 and 817 cells L^{-1}, respectively). In addition to seasonal effects, the variations in dinoflagellate numbers could also be attributed to the difference in sampling coverage, as more areas with shallow waters were sampled in this study and higher abundance of dinoflagellates has often been observed in estuarine and coastal waters than in shelf and slope waters in the nSCS (Lan et al., 2009; Wei et al., 2018). The high number of dinoflagellates in this study is mainly due to highly abundant *Akashiwo* cf. *sanguinea* (MTD) and *Katodinium* sp. (HTD) in the coastal waters. Relative to the higher abundance of dinoflagellates, the species richness of dinoflagellates recorded in our study was lower than that reported by Ke et al. (2011) in summer. However, some dinoflagellate species occurred in both studies, such as *A.* cf. *sanguinea*, *Ceratium furca*, *C. fusus*, *C. macroceros*, *C. teres*, *Dinophysis caudata*, *Prorocentrum micans*, *P. sigmoides*, and *Noctiluca scintillans*, suggesting that these are eurythermal species and may occur in the nSCS throughout the year.

In spite of the differences mentioned above regarding both ciliates and dinoflagellates, the horizontal distribution pattern, characterised by a decreasing trend from the nearshore to offshore areas in our study, was consistent with the findings of previous studies (Liu et al., 2010; Ke et al., 2011; Zheng et al., 2012; Yu et al., 2014; Wei et al., 2018) and has also been commonly found in other marine regions (Santoferrara et al., 2011; Jiang et al., 2014; Yang et al., 2020a). Owing to the effect of the runoff from the Pearl River, a large amount of terrestrial nutrients is brought into the Pearl River Estuary and its adjacent coastal waters in the nSCS. In addition, under the influence of the northeast monsoon in winter, high nutrient coastal water enters the SCS from the East China Sea through the Taiwan Strait, forming a southwest coastal current along the northern coast of the SCS (Fang et al., 1998). These complex physical processes all bring plenty of nutrients to the northern coast of the SCS and, thus, maintain the Chl *a* concentration at a high level along the coast (Hao et al., 2011), resulting in an increase in food sources for microzooplankton grazers and a decreasing trend of microzooplankton distribution from coastal to shelf and slope areas.

4.2. Insights into the functioning of microzooplankton and potential risk of HABs

Microzooplankton are known to have three major trophic modes (i.e. strongly autotrophic mixotrophs, mixotrophs, and heterotrophs) and play diverse roles in marine planktonic food webs (Johnson, 2011; Yang et al., 2020b). The strongly autotrophic red *Mesodinium* spp. can contribute to a substantial part of primary production, and mixotrophic and heterotrophic microzooplankton are able to feed on diverse types and sizes of prey and also serve as excellent prey for phagotrophic protists and metazoans (Jeong et al., 2010; Stoecker et al., 2017). Our results showed a high abundance and proportion of red *Mesodinium* spp.
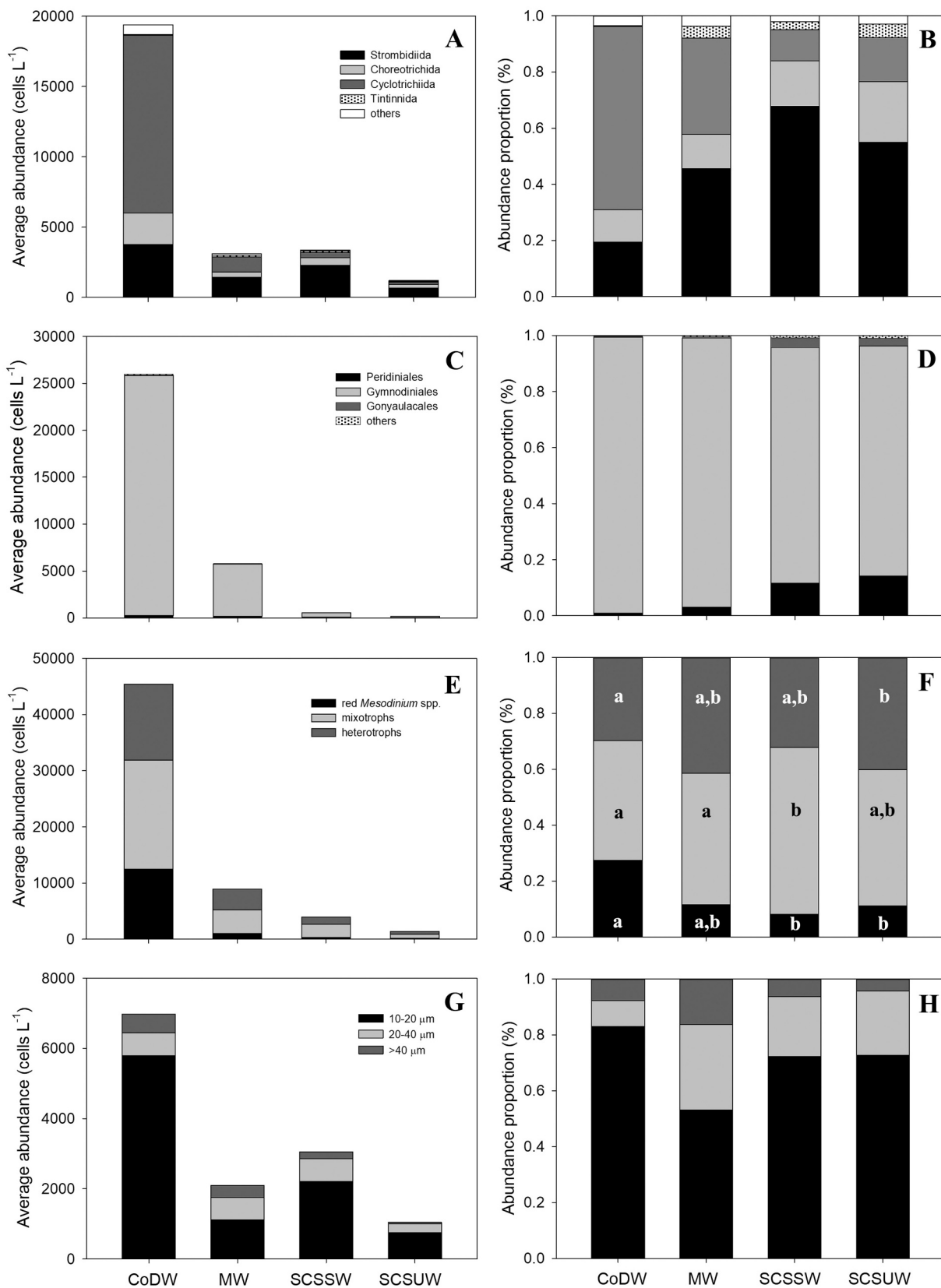
Fig. 7. Average abundance and proportions of ciliates (A, B), dinoflagellates (C, D), and different functional groups (E, F) in the microzooplankton communities and different size (equivalent spherical diameter, ESD) groups (G, H) of ciliated grazers in the four water masses. Different lowercase letters indicate significant differences ($P < 0.05$) between the water masses.

in the CoDW (Fig. 7E, F) because of the abundance of *M. rubrum* in the waters, suggesting that they may constitute an essential part of the high chlorophyll biomass in the coastal waters of the nSCS (Hao et al., 2011; Yu et al., 2014). In contrast, the larger species, *M. major*, which often dominates ciliate biomass in the plankton in coastal temperate waters together with *M. rubrum* (Yang et al., 2015; Stoecker et al., 2017), were relatively rare in this study. A study on the temporal distribution of red *Mesodinium* spp. and its driving factors in the nSCS is necessary to better understand their function in the system.

The mixotrophs dominated the microzooplankton communities in all the water masses, especially in the SCSSW, indicating that the environmental conditions might be favourable for the mixotrophs, which have trophic flexibility and obtain sustenance from light, dissolved inorganic nutrients, and ingestion (Jeong et al., 2010; Stoecker et al., 2017). In the SCSSW and SCSUW, the mixotrophs were mainly composed of chloroplast-retaining oligotrich ciliates with acquired phototrophy owing to the sequestration of functional plastids from phytoplankton prey (Johnson, 2011). In the CoDW and MW, the unarmoured dinoflagellate *A.* cf. *sanguinea* was the most dominant mixotrophic microzooplankton in the waters. The distribution of *A. sanguinea* could be related to its mixotrophy ability, which may help balance its nitrogen requirements and give this species an advantage over other trophic groups (Bockstahler and Coats, 1993). It is known that *A. sanguinea* can feed on diverse taxa (Jeong et al., 2010) and appears to feed preferentially on nano-sized oligotrichous ciliates, by which they may reverse the normal material flow from the primary producer to the consumer, thereby affecting the trophodynamics of the microbial food web in the system (Bockstahler and Coats, 1993).

The proportion of heterotrophs in the SCSUW was significantly higher than that in the CoDW. The weak light condition in subsurface waters may give heterotrophs a certain advantage in competition with mixotrophs because the maximum growth rates of heterotrophic microzooplankton are normally higher than those of mixotrophs when growing under low light conditions (Jeong et al., 2010). The size-fractionated compositions of ciliated grazers showed that nano-sized ciliates were the most abundant in all the water masses (Fig. 7G, H), indicating a close trophic coupling between ciliates and picoplankton in the nSCS ecosystem (Hansen et al., 1997; Thurman et al., 2010). The variations in the spatial distribution patterns of ciliates and dinoflagellates suggest that they may play different roles in structuring the plankton communities in the nSCS, as revealed in a temperate water system by Yang et al. (2020b). The top-down control effect by dinoflagellates may have a substantial effect on the inshore region where diatoms are often abundant. Xiao et al. (2018), who used decadal-scale phytoplankton pigment data to test whether realised traits could explain the biogeographic patterns of phytoplankton variability in tropical and subtropical marginal seas, reported that similar realised traits were found for diatoms and dinoflagellates, which were dominant together in coastal waters characterised by low salinity and high concentrations of nutrients. In the offshore region, where phytoflagellates and cyanobacteria are dominant in the phytoplankton communities (Zhai et al., 2011; Xiao et al., 2018), the grazing impact by ciliates may be predominant in the waters.

It is known that *A.* cf. *sanguinea* is a harmful red-tide-forming MTD (Tang and Gobler, 2015) and the high abundance of it in the upper waters along the coast indicated a potential risk of HABs in the nSCS during early spring. The large MTD *A. sanguinea* is cosmopolitan and frequently forms HABs in surface waters from temperate to tropical estuaries and coasts around the world, with cell densities often exceeding 1×10^5 cells L^{-1} as in this study or even higher (Lu and Hodgkiss, 2004; Tang and Gobler, 2015). However, HABs resulting from *A. sanguinea* have not been as frequently reported as those by *Phaeocystis globosa* in the nSCS (Lu and Hodgkiss, 2004; Glibert et al., 2018). A high abundance of *A. sanguinea* may be related to high nutrients and sufficient food sources (Fig. 7G) in coastal waters (Bockstahler and Coats, 1993; Tang and Gobler, 2015). In addition, *A. sanguinea* can tolerate a wide range of temperatures and salinities, and their resting cysts can accumulate in sediments and are resistant to harsh environments (Tang and Gobler, 2015). In the past few decades, HABs in China have undergone significant changes with the bloom-forming species becoming increasingly diversified, and the blooms shifting from diatoms to flagellates that tend to be harmful (Glibert et al., 2018). Given that *A. sanguinea* blooms may pose a significant threat to the fish and shellfish mariculture industry and other marine animals, it is important to monitor their risk of occurrence and understand the mechanisms regulating their distribution and formation.

4.3. Potential for microzooplankton communities to be indicators for discriminating water masses in the nSCS

Planktonic ciliates have been used as potential indicators of aquatic environments in recent years because of their limited mobility, ease of sampling, wide distribution, and increasing availability of taxonomic references (Jiang et al., 2016). For example, investigations on the spatial distributions of pelagic ciliate communities in the Amundsen Sea (Antarctica) and the western Arctic Ocean revealed significant differences among the various habitats in terms of community structure, abundance, biomass, and biodiversity indices (Jiang et al., 2013, 2014, 2016). Yang et al. (2020a) studied the spatial distribution patterns of planktonic ciliate communities in the coastal and continental regions of the East China Sea in summer and suggested that they could be used as potential indicators of water masses in marine systems with dynamic environmental variations. However, the relationships between the spatial distribution patterns of whole microzooplankton communities and environmental variations have not been well addressed.

The results of the present study clearly showed that the microzooplankton community structure, including dominant species and diversity indices, was closely correlated with the hydrological structure of the coastal and continental shelf regions in the nSCS and could be potential indicators of water masses. Although significant differences in microzooplankton abundance and biomass among different water masses were revealed in the present study, their effectiveness in discriminating between two water masses was unsatisfactory according to the LSD test, suggesting that it is not practical to detect environmental variations unambiguously based on total microzooplankton abundance and/or biomass alone. With the help of a multivariate analysis on community composition based on species and abundance data, the spatial distribution patterns of microzooplankton communities in the different water masses could be well discriminated (Fig. 6; Table 1), indicating the effectiveness of using microzooplankton communities as potential indicators of water masses. Although biological indicators may not be as sensitive as physico-chemical indicators because the biota cannot react as quickly and directly as physico-chemical parameters to environmental variations, they can provide vital information on the functional structure and reflect the overall and comprehensive situation of the ecosystem. Future studies are needed to test the effectiveness in other seasons, both in the nSCS and in other marine systems.

5. Conclusion

The present study revealed that microzooplankton communities in the western nSCS were dominated by cyclotrichids (mainly *M. rubrum*), aloricate oligotrichs, and choreotrichs within ciliates and the order Gymnodiniales within dinoflagellates and exhibited a decreasing trend from coastal to continental shelf areas. Significant differences in the spatial distribution of microzooplankton were found among the water masses in terms of both abundance and carbon biomass, with the highest mean values in the CoDW and the lowest in the SCSUW. A multivariate correlation analysis revealed clear spatial patterns in microzooplankton community structure, diversity indices, and dominant species among the different water masses. An analysis of the trophic compositions of microzooplankton communities showed that a relatively high

proportion of red *Mesodinium* spp. occurred in the CoDW and the mixotrophs dominated in all the water masses, which may lead to greater recycling of inorganic nutrients. Small-sized ciliates dominated the ciliate communities in all the water masses, while large-sized ciliates comprised a relatively higher proportion in the MW that in the other water masses. Moreover, our results indicated a potential risk of HABs of the MTD *A. sanguinea* along the coast of the nSCS during early spring. This study provides basic data and strong evidence on the effectiveness of using microzooplankton communities as potential indicators of water masses in marine systems with dynamic environmental variations.

Supplementary data to this article can be found online at https://doi.org/10.1016/j.marpolbul.2020.111898.

CRediT authorship contribution statement

Jinpeng Yang: Conceptualization, Formal analysis, Writing - original draft, Funding acquisition. **Zijian Chen:** Formal analysis, Investigation. **Dongxing Chen:** Formal analysis. **Dapeng Xu:** Writing - original draft, Funding acquisition.

Declaration of competing interest

The authors declare that they have no known competing financial interests or personal relationships that could have appeared to influence the work reported in this paper.

References

Anderson, M.J., Gorley, R.N., Clarke, K.R., 2008. PERMANOVA+ for PRIMER Guide to Software and Statistical Methods. PRIMER-E Ltd, Plymouth.

Azam, F., Fenchel, T., Field, J.G., Gray, J.S., Meyer-Reil, L.A., Thingstad, F., 1983. The ecological role of water-column microbes in the sea. Mar. Ecol. Prog. Ser. 10, 257–263.

Berge, T., Hansen, P.J., Moestrup, Ø., 2008. Feeding mechanism, prey specificity and growth in light and dark of the plastidic dinoflagellate *Karlodinium armiger*. Aquat. Microb. Ecol. 50, 279–288.

Bockstahler, K.R., Coats, D.W., 1993. Grazing of the mixotrophic dinoflagellate *Gymnodinium sanguineum* on ciliate populations of Chesapeake Bay. Mar. Biol. 116, 477–487.

Burkill, P.H., Edwards, E.S., John, A.W.G., Sleigh, M.A., 1993. Microzooplankton and their herbivorous activity in the northeastern Atlantic Ocean. Deep-Sea Res. II 40, 479–493.

Capriulo, G.M., Sherr, E.B., Sherr, B.F., 1991. Trophic behaviour and related community feeding activities of heterotrophic marine protists. In: Reid, P.C., Turley, C.M., Burkill, P.H. (Eds.), Protozoa and their Role in Marine Processes. Springer, Berlin, pp. 219–265.

Clarke, K.R., Gorley, R.N., 2006. PRIMER 6: User Manual/Tutorial. PRIMER-E Ltd, Plymouth.

Dai, S., Zhao, Y.F., Liu, H.J., Hu, Z.Y., Zheng, S., Zhu, M.L., Guo, S.J., Sun, X.X., 2020. The effects of a warm-core eddy on chlorophyll a distribution and phytoplankton community structure in the northern South China Sea in spring 2017. J. Mar. Syst. 210, 103396.

Fang, G.H., Fang, W.D., Fang, Y., Wang, K., 1998. A survey of studies on the South China Sea upper ocean circulation. Acta Oceanogr. Taiwan 37, 1–16.

Gan, J.P., Lu, Z.M., Dai, M.H., Cheung, A.Y.Y., Liu, H.B., Harrison, P., 2010. Biological response to intensified upwelling and to a river plume in the northeastern South China Sea: a modeling study. J. Geophys. Res. 115, C09001.

Garrison, D.L., Gibson, A., Coale, S.L., Gowing, M.M., Okolodkov, Y.B., Fritsen, C.H., Jeffries, M., 2005. Sea-ice microbial communities in the Ross Sea: autumn and summer biota. Mar. Ecol. Prog. Ser. 300, 39–52.

Gifford, D.J., 1991. The protozoan-metazoan trophic link in pelagic ecosystems. J. Protozool. 38, 81–86.

Glibert, P.M., Berdalet, E., Burford, M.A., Pitcher, G.C., Zhou, M.J., 2018. Global Ecology and Oceanography of Harmful Algal Blooms. Springer.

Hansen, P.J., 1991. Quantitative importance and trophic role of heterotrophic dinoflagellates in a coastal pelagial food web. Mar. Ecol. Prog. Ser. 73, 253–261.

Hansen, P.J., Bjørnsen, P.K., Hansen, B.W., 1997. Zooplankton grazing and growth: scaling within the 2-2,000 μm body size range. Limnol. Oceanogr. 42, 687–704.

Hao, Q., Ning, X.R., Liu, C.G., Le, F.F., 2011. The physical-biological oceanography coupling characteristics of primary production in the northern South China Sea and the influences on carbon fixation. J. Mar. Sci. 29, 46–57.

Hillebrand, H., Dürselen, C.D., Kirschtel, D., Pollingher, U., Zohary, T., 1999. Biovolume calculation for pelagic and benthic microalgae. J. Phycol. 35, 403–424.

Huang, H.C., Yang, J.P., Huang, S.X., Gu, B.W., Wang, Y., Wang, L., Jiao, N.Z., Xu, D.P., 2020. Spatial distribution of planktonic ciliates in the western Pacific Ocean: along the transect from Shenzhen (China) to Pohnpei (Micronesia). Mar. Life Sci. Tech. https://doi.org/10.1007/s42995-020-00075-7.

Jeong, H.J., 1999. The ecological roles of heterotrophic dinoflagellates in marine planktonic community. J. Eukaryot. Microbiol. 46, 390–396.

Jeong, H.J., Park, J.Y., Nho, J.H., Park, M.O., Ha, J.H., Seong, K.A., Jeng, C., Seong, C.N., Lee, K.Y., Yih, W.H., 2005. Feeding by red-tide dinoflagellates on the cyanobacterium *Synechococcus*. Aquat. Microb. Ecol. 41, 131–143.

Jeong, H.J., Song, J.E., Kang, N.S., Kim, S., Yoo, Y.D., Park, J.Y., 2007. Feeding by heterotrophic dinoflagellates on the common marine heterotrophic nanoflagellate *Cafeteria* sp. Mar. Ecol. Prog. Ser. 333, 151–160.

Jeong, H.J., Seong, K.A., Yoo, Y.D., Kim, T.H., Kang, N.S., Kim, S., Park, J.Y., Kim, J.S., Kim, G.H., Song, J.Y., 2008. Feeding and grazing impact by small marine heterotrophic dinoflagellates on heterotrophic bacteria. J. Eukaryot. Microbiol. 55, 271–288.

Jeong, H.J., Yoo, Y.D., Kim, J.S., Seong, K.A., Kang, N.S., Kim, T.H., 2010. Growth, feeding and ecological roles of the mixotrophic and heterotrophic dinoflagellates in marine planktonic food webs. Ocean Sci. J. 45, 65–91.

Jiang, Y., Yang, E.J., Min, J.O., Kang, S.H., Lee, S.H., 2013. Using pelagic ciliated microzooplankton communities as an indicator for monitoring environmental condition under impact of summer sea-ice reduction in western Arctic Ocean. Ecol. Indic. 34, 380–390.

Jiang, Y., Yang, E.J., Kim, S.Y., Kim, Y.N., Lee, S.H., 2014. Spatial patterns in pelagic ciliate community responses to various habitats in the Amundsen Sea (Antarctica). Prog. Oceanogr. 128, 49–59.

Jiang, Y., Liu, Q., Yang, E.J., Wang, M., Kim, T.W., Cho, K.H., Lee, S.H., 2016. Pelagic ciliate communities within the Amundsen Sea polynya and adjacent sea ice zone, Antartica. Deep-Sea Res. II 123, 69–77.

Johnson, M.D., 2011. Acquired phototrophy in ciliates: a review of cellular interactions and structural adaptations. J. Eukaryot. Microbiol. 58, 185–195.

Ke, Z.X., Huang, L.M., Tan, Y.H., Yin, J.Q., 2011. Species composition and abundance of phytoplankton in the northern South China Sea in summer 2007. J. Trop. Oceanogr. 30, 131–143.

Kofoid, C.A., Campbell, A.S., 1929. A conspectus of the marine and freshwater Ciliata belonging to the suborder Tintinnoinea, with descriptions of new species principally from the Agassiz expedition to the eastern tropical Pacific 1904–1905. Univ. Calif. Publ. Zool. 34, 1–403.

Kraberg, A.C., Baumann, M., Dürselen, C.D., 2010. Coastal Phytoplankton-Photo Guide for Northern European Seas. Verlag Dr. Freidrich, Pfeil, München.

Lan, W.L., Huang, B.Q., Dai, M.H., Ning, X.R., Huang, L.F., Hong, H.S., 2009. Dynamics of heterotrophic dinoflagellates off the Pearl River Estuary, northern South China Sea. Estuar. Coast. Shelf Sci. 85, 422–430.

Landry, M.R., Calbet, A., 2004. Microzooplankton production in the oceans. ICES J. Mar. Sci. 61, 501–507.

Levinsen, H., Nielsen, T.G., 2002. The trophic role of marine pelagic ciliates and heterotrophic dinoflagellates in arctic and temperate coastal ecosystems: a cross-latitude comparison. Limnol. Oceanogr. 47, 427–439.

Li, A., Stoecker, D.K., Coats, D.W., 2000. Mixotrophy in *Gyrodinium galatheanum* (Dinophyceae): grazing responses to light intensity and inorganic nutrients. J. Phycol. 36, 33–45.

Li, L., Li, F.Q., Su, J., Xu, J.P., 2002. Analysis on water masses in the South China Sea in summer and winter of 1998. Oceanol. Limnol. Sin. 33, 393–401.

Liang, W.D., Yang, Y.J., Tang, T.Y., Chuang, W.S., 2008. Kuroshio in the Luzou Strait. J. Geophys. Res. 113, C08048.

Liu, H.X., Tan, Y.H., Huang, L.M., Song, X.Y., Huang, J.R., Li, T., 2010. Composition and distribution of ciliates in northern South China Sea during summer. Acta Ecol. Sin. 30, 2340–2346.

Löder, M.G.J., Meunier, C., Wiltshire, K.H., Boersma, M., Aberle, N., 2011. The role of ciliates, heterotrophic dinoflagellates and copepods in structuring spring plankton communities at Helgoland Roads, North Sea. Mar. Biol. 158, 1551–1580.

Löder, M.G.J., Kraberg, A.C., Aberle, N., Peters, S., Wiltshire, K.H., 2012. Dinoflagellates and ciliates at Helgoland Roads, North Sea. Helgol. Mar. Res. 66, 11–23.

Lu, S.H., Hodgkiss, I.J., 2004. Harmful algal bloom causative collected from Hong Kong waters. Hydrobiologia 512, 231–238.

Menden-Deuer, S., Lessard, E.J., 2000. Carbon to volume relationships for dinoflagellates, diatoms, and other protist plankton. Limnol. Oceanogr. 45, 569–579.

Montagnes, D.J.S., Lynn, D.H., 1991. Taxonomy of the major groups of marine planktonic ciliates, with emphasis on the aloricate forms. Mar. Microb. Food Webs 5, 59–74.

Nakamura, Y., Suzuki, S., Hiromi, J., 1995. Population dynamics of heterotrophic dinoflagellates during a *Gymnodinium mikimotoi* red tide in the Seto Inland Sea. Mar. Ecol. Prog. Ser. 125, 269–277.

Putt, M., Stoecker, D.K., 1989. An experimentally determined carbon: volume ratio for marine "oligotrichous" ciliates from estuarine and coastal waters. Limnol. Oceanogr. 34, 1097–1103.

Qi, Y.Z., Chen, J.F., Wang, Z.H., Xu, N., Wang, Y., Shen, P.P., Lu, S., Hodgkiss, I.J., 2004. Some observations on harmful algal bloom (HAB) events along the coast of Guangdong, southern China in 1998. Hydrobiologia 512, 209–214.

Reid, F.M.H., Stewart, E., 1989. Nearshore microplanktonic assemblages off southern California in February 1983 during the El Niño event. Cont. Shelf Res. 9, 37–50.

Santoferrara, L.F., Gomez, M.I., Alder, V.A., 2011. Bathymetric, latitudinal and vertical distribution of protozooplankton in a cold-temperate shelf (southern Patagonian waters) during winter. J. Plankton Res. 33, 457–468.

Sherr, E.B., Sherr, B.F., 1987. High rates of consumption of bacteria by pelagic ciliates. Nature 325, 710–711.

Sherr, E.B., Sherr, B.F., Ross, C., 2013. Microzooplankton grazing impact in the Bering Sea during spring sea ice conditions. Deep-Sea Res. II 94, 57–67.

Song, W.B., Warren, A., Hu, X.Z., 2009. Free-living Ciliates in the Bohai and Yellow Seas, China. Science Press, Beijing.

Stoecker, D.K., 1999. Mixotrophy among dinoflagellates. J. Eukaryot. Microbiol. 46, 397–401.

Stoecker, D.K., Hansen, P.J., Caron, D.A., Mitra, A., 2017. Mixotrophy in the marine plankton. Annu. Rev. Mar. Sci. 9, 311–335.

Sun, P., Huang, L.Y., Xu, D.P., Huang, B.Q., Chen, N., Warren, A., 2017. Marked seasonality and high spatial variation in estuarine ciliates are driven by exchanges between the "abundant" and "intermediate" biospheres. Sci. Rep. 7, 9494.

Sun, P., Huang, L.Y., Xu, D.P., Warren, A., Huang, B.Q., Wang, Y., Wang, L., Xiao, W.P., Kong, J., 2019. Integrated space-time dataset reveals high diversity and distinct community structure of ciliates in mesopelagic waters of the northern South China Sea. Front. Microbiol. 10, 2178.

Sun, P., Wang, Y., Laws, E., Huang, B.Q., 2020. Water mass-driven spatial effects and environmental heterogeneity shape microeukaryote biogeography in a subtropical, hydrographically complex ocean system – a case study of ciliates. Sci. Total Environ. 706, 135753.

Tang, Y.Z., Gobler, C.J., 2015. Sexual resting cyst production by the dinoflagellate Akashiwo sanguinea: a potential mechanism contributing to the ubiquitous distribution of a harmful alga. J. Phycol. 51, 298–309.

Tang, D.L., Kester, D.R., Ni, I.H., Qi, Y.Z., Kawamura, H., 2003. In situ and satellite observations of a harmful algal bloom and water condition at the Pearl River estuary in late autumn 1998. Harmful Algae 2, 89–99.

Thurman, J., Parry, J.D., Hill, P.J., Laybourn-Parry, J., 2010. The filter feeding ciliates *Colpidium striatum* and *Tetrahymena pyriformis* display selective feeding behaviours in the presence of mixed, equally-sized, bacterial prey. Protist 161, 577–588.

Tillmann, U., 2004. Interactions between planktonic microalgae and protozoan grazers. J. Eukaryot. Microbiol. 51, 156–168.

Wang, S.F., Tang, D.L., He, F.L., Fukuyo, Y., Azanza, R.V., 2008. Occurrences of harmful algal blooms (HABs) associated with ocean environments in the South China Sea. Hydrobiologia 596, 79–93.

Wang, C.F., Li, H.B., Zhao, L., Zhao, Y., Dong, Y., Zhang, W.C., Xiao, T., 2019. Vertical distribution of planktonic ciliates in the oceanic and slope areas of the western Pacific Ocean. Deep-Sea Res. II 167, 70–78.

Wei, N., Satheeswaran, T., Jenkinson, I.R., Xue, B., Wei, Y.Q., Liu, H.J., Sun, J., 2018. Factors driving the spatiotemporal variability in phytoplankton in the Northern South China Sea. Cont. Shelf Res. 162, 48–55.

Wickham, S.A., Steinmair, U., Kamennaya, N., 2011. Ciliate distributions and forcing factors in the Amundsen and Bellingshausen Seas (Antarctic). Aquat. Microb. Ecol. 62, 215–230.

Wu, R.S., Li, L., 2003. Summarization of study on upwelling system in the South China Sea. J. Oceanogr. Taiwan Strait 22, 269–277.

Xiao, W.P., Wang, L., Laws, E., Xie, Y.Y., Chen, J.X., Liu, X., Chen, B.Z., Huang, B.Q., 2018. Realized niches explain spatial gradients in seasonal abundance of phytoplankton groups in the South China Sea. Prog. Oceanogr. 162, 223–239.

Yang, J.P., Löder, M.G.J., Gerdts, G., Wiltshire, K.H., 2015. Structural composition and temporal variation of the ciliate community in relation to environmental factors at Helgoland Roads, North Sea. J. Sea Res. 101, 19–30.

Yang, J.P., Löder, M.G.J., Jiang, Y., Wiltshire, K.H., 2019. Are tintinnids picky grazers: feeding experiments on a mixture of mixotrophic dinoflagellates and implications for red tide dynamics. Mar. Pollut. Bull. 149, 110488.

Yang, J.P., Huang, S.X., Fan, W.X., Warren, A., Jiao, N.Z., Xu, D.P., 2020a. Spatial distribution patterns of microzooplankton communities in the South China Sea: potential indicators of water masses. Mar. Pollut. Bull. 156, 111253.

Yang, J.P., Löder, M.G.J., Gerdts, G., Wiltshire, K.H., Montagnes, D.J.S., 2020b. Comparing the trophic impact of microzooplankton during the spring and autumn blooms in temperate waters. Estuar. Coast. 6 https://doi.org/10.1007/s12237-020-00775-4.

Yoo, Y.D., Jeong, H.J., Kim, M.S., Kang, N.S., Song, J.Y., Shin, W.G., Kim, K.Y., Lee, K.T., 2009. Feeding by phototrophic red-tide dinoflagellates on the ubiquitous marine diatom *Skeletonema costatum*. J. Eukaryot. Microbiol. 56, 413–420.

Yu, Y., Zhang, W.C., Cai, Y.M., Feng, M.P., Li, H.B., Xiao, T., 2014. Distribution patterns of planktonic ciliates in the northern South China Sea in winter and summer, 2009. Oceanol. Limnol. Sin. 45, 839–847.

Zhai, H.C., Ning, X.R., Tang, X.X., Hao, Q., Le, F.F., Qiao, J., 2011. Phytoplankton pigment patterns and community composition in the northern South China Sea during winter. Chin. J. Oceanol. Limn. 29, 233–245.

Zheng, L.P., Xaing, W.G., Huang, B.Q., 2012. Grazing pressure of microzooplankton on phytoplankton in northern South China Sea in winter. J. Oceanogr. Taiwan Strait 31, 72–78.